

# Testing a string dilaton model with experimental and observational data

Susana J.Landau<sup>1,2</sup> \*    Melina Bersten<sup>1,3</sup> †    Pablo Sisterna ‡

Hector Vucetich<sup>1</sup> §

<sup>1</sup> Facultad de Ciencias Astronómicas y Geofísicas,  
Universidad Nacional de La Plata

Paseo del Bosque S/N, CP 1900 La Plata, Argentina

<sup>2</sup> Departamento de Física, Facultad de Ciencias Exactas y Naturales,  
Universidad Nacional de Buenos Aires

Pabellón I, Ciudad Universitaria, 1428, Buenos Aires, Argentina

<sup>3</sup> Departamento de Astronomía y Astrofísica  
Pontificia Universidad Católica de Chile

Av. Vicuña Mackenna 4860, 782-0436 Macul, Santiago, Chile

May 11, 2019

We test the prediction of the time variation of the fine structure constant in the string dilaton model proposed by Damour and Polyakov. First, we analyze the dependence of all available observational and experimental data with the fine structure constant variation. Furthermore, we obtain the prediction of the time variation of the fine structure constant including the renormalization group correction. Finally, we use the data set to perform a statistical analysis. This analysis enables us to determine that the dilaton model is in agreement with most of the data. Finally, constraints on the free parameters of this model are obtained.

---

\*e-mail: [slandau@df.uba.ar](mailto:slandau@df.uba.ar)

†e-mail: [mbersten@astro.puc.cl](mailto:mbersten@astro.puc.cl)

‡e-mail: [sisterna@museodelmar.org](mailto:sisterna@museodelmar.org)

§e-mail: [vucetich@fcaglp.unlp.edu.ar](mailto:vucetich@fcaglp.unlp.edu.ar)

## 1 Introduction

The attempt to unify all fundamental interactions resulted in the development of multidimensional theories like string derived field theories [1, 2, 3, 4, 5, 6], related brane-world theories [7, 8, 9, 10], and (related or not) Kaluza-Klein theories [11, 12, 13, 14, 15]. Among these theories, there are some in which the gauge coupling constants may vary over cosmological time scales. On the other hand, a theoretical framework based on first principles, was developed by Bekenstein [16] and later improved by Barrow, Sandvik and Magueijo [17] in order to study the possible time variation of the fine structure constant. Furthermore, this model was generalized to study the variation of the strong coupling constant by Chamoun et al.[18].

Different versions of the theories mentioned above predict different time behaviours of the gauge coupling constants. Thus, bounds obtained from astronomical and geophysical data are an important tool to test the validity of these theories.

The experimental research can be grouped into astronomical and local methods. The latter ones include geophysical methods such as the natural nuclear reactor that operated about  $1.8 \cdot 10^9$  years ago in Oklo, Gabon [19, 20, 21], the analysis of natural long-lived  $\beta$  decayers in geological minerals and meteorites [22, 23, 24] and laboratory measurements such as comparisons of rates between clocks with different atomic number [25, 26, 27, 28, 29, 30]. The astronomical methods are based mainly in the analysis of spectra from high-redshift quasar absorption systems [31, 32, 33, 34, 35, 36, 37, 38, 39, 40, 41]. Although, most of the previous mentioned experimental data gave null results, evidence of time variation of the fine structure constant was reported recently from high-redshift quasar absorption systems [33, 34, 35, 36, 39, 40]. However, other recent independent analysis of similar data [41, 42, 43, 44] found no variation. On the other hand, measurements of molecular hydrogen [38, 40] reported a variation of the proton to electron mass  $\mu = \frac{m_p}{m_e}$ . Furthermore, the time variation of the gauge coupling constants in the early universe can be constrained using data from the Cosmic Microwave Background (CMB) [45, 46, 47, 48] and the primordial abundances of light elements [49, 50, 51].

Damour and Polyakov [4] proposed a string dilaton model in which the variation of the gauge coupling constants is driven by the time evolution of the dilaton field. In this model, the dilaton remains massless and in consequence all coupling constants and masses of elementary particles are time dependent. In this chapter we limit ourselves to the variation of the fine structure constant. We compare the prediction of the dilaton model with

all available data on time variation of the fine structure constant but the nucleosynthesis data. In section 2 we describe carefully the data set considered. In section 3 we briefly review the Damour and Polyakov proposal [4] and obtain the analytic expression for the prediction of the time variation of the fine structure constant including the renormalization group corrections. Finally, in section 4 we present the results of the statistical analysis and briefly discuss our conclusions.

## 2 Bounds from astronomical and geophysical data

In this section, we review all available bounds on time variation of the fine structure constant. We discuss the relation between the observable quantities and the variation of  $\alpha$  in each case. We also describe very carefully the error we consider for each data.

### 2.1 The Oklo Phenomenon

One of the most stringent limits on time variation of the fine structure constant  $\alpha$  follows from an analysis of isotope ratios in the natural uranium fission reactor that operated  $1.8 \times 10^9$  yrs ago at the present day site of the Oklo mine in Gabon, Africa. From an analysis of nuclear and geochemical data, the operating conditions of the reactor could be reconstructed and the thermal neutron capture cross sections of several nuclear species measured. In particular, a shift in the lowest lying resonance level in  $^{149}\text{Sm}$ :  $\Delta = E_r^{149(\text{Oklo})} - E_r^{149(\text{now})}$  can be derived from a shift in the neutron capture cross section of the same nucleus [20, 19]. The first estimate of a change in the resonance energy was performed by Damour and Dyson [19]. This bound was re-examined by Fujii et al [20] using new samples of  $^{149}\text{Sm}$ ,  $^{155}\text{Gd}$  and  $^{157}\text{Gd}$ . In their analysis they take the effect of contamination into account, assuming the same contamination parameter for all samples. They obtain the following bound:

$$\Delta = E_r^{Oklo} - E_r^{today} = (9 \pm 11) 10^{-3} eV \quad (1)$$

The shift in  $\Delta$  can be translated [19] into a bound on a possible difference between the value of  $\alpha$  during the Oklo phenomenon and its value now, as follows:

$$\Delta = \alpha \frac{\partial E_r}{\partial \alpha} \frac{\Delta \alpha}{\alpha} \quad (2)$$

where  $\frac{\partial E_r}{\partial \alpha} = 10^6$ . The dependence of the resonance energy with other fundamental constants has been analyzed by Damour and Dyson [19] and Sisterna and Vucetich [52].

## 2.2 Long-lived $\beta$ decayers

The half-life of long-lived  $\beta$  decayers has been determined either in laboratory measurements or by comparison with the age of meteorites, as found from  $\alpha$  decay radioactivity analysis. In table 2.2, we show  $\frac{\Delta\lambda}{\lambda}$  for three different decayers:  $^{187}\text{Re}$ ,  $^{40}\text{K}$ ,  $^{87}\text{Rb}$ . Sisterna and Vucetich [23] have derived a relation between the shift in the half-life of long lived  $\beta$  decayers and a possible variation between the values of the fundamental constants  $\alpha$ ,  $\Lambda_{QCD}$  and  $G_F$  at the age of the meteorites and their value now. In this chapter, we only consider  $\alpha$  variation and therefore, the following equation holds:

$$\frac{\Delta\lambda}{\lambda} = a \frac{\Delta\alpha}{\alpha} \quad (3)$$

where  $a = 21600, 46, 1070$  for  $^{187}\text{Re}$ ,  $^{40}\text{K}$ ,  $^{87}\text{Rb}$  respectively [52].

Table 1: The table shows the  $\beta$  decayer, the difference of half life measured in the laboratory and from meteorites, the corresponding error and reference.

$\beta$ decayer	$\frac{\Delta\lambda}{\lambda}$	$\sigma\left(\frac{\Delta\lambda}{\lambda}\right)$	Reference
$^{187}\text{Re}$	$-1.6 \cdot 10^{-2}$	$1.6 \cdot 10^{-2}$	[24]
$^{40}\text{K}$	0	$1.3 \cdot 10^{-2}$	[22]
$^{87}\text{Rb}$	0	$1.3 \cdot 10^{-2}$	[22]

## 2.3 Atomic clocks

The comparison of different atomic transition frequencies over time can be used to determine the present value of the temporal derivative of  $\alpha$ . Indeed, the more stringent limits on the variation of  $\alpha$  are obtained using this method.

Hyperfine transition frequencies have the following dependence with  $\alpha$ :

$$\nu_{Hyp} \sim \alpha^2 \frac{\mu}{\mu_N} \frac{m_e}{m_p} R_\infty c F_{REL}(\alpha Z) \quad (4)$$

where  $\mu$  is the nuclear magnetic moment,  $\mu_B$  is Bohr magneton,  $R_\infty$  is Rydberg's constant,  $m_p$  and  $m_e$  are the proton and electron mass and  $F_{REL}$

is the relativistic contribution to the energy. In such way, the comparison of rates between clocks based on hyperfine transitions in alkali atoms with different atomic number  $Z$  can be used to set bounds on  $\alpha^k \frac{\mu_{A_1}}{\mu_{A_2}}$  where  $k$  depends on the frequencies measured and  $\mu_{A_i}$  refers to the nuclear magnetic moment of each atom. As explained above, we are considering only  $\alpha$  variation, but it is important to keep in mind that this type of experiments actually constrain a combination of  $\alpha$  and other fundamental quantities. The first three entries of table 2.3 show the bounds on  $\frac{\Delta\alpha}{\alpha}$  obtained comparing hyperfine transition frequencies in alkali atoms. On the other hand, an optical transition frequency has a different dependence on  $\alpha$ :

$$\nu_{opt} \sim R_{\infty} B F_i(\alpha) \quad (5)$$

where  $B$  is a numerical constant assumed not to vary in time and  $F_i(\alpha)$  is a dimensionless function of  $\alpha$  that takes into account level shifts due to relativistic effects. Thus, comparing an optical transition frequency with an hyperfine transition frequency can be used to set bound on  $\alpha^k \frac{m_e \mu_A}{m_p \mu_B}$ . Again, we will only consider  $\alpha$  variation. Different authors [28, 29, 30] have measured different optical transitions and set bounds on the variation of  $\alpha$  using different methods. Fischer et al [29] have considered the joint variation of  $\alpha$  and  $\frac{\mu_{Cs}}{\mu_B}$ . We have reanalyzed the data of ref. [29], considering only  $\alpha$  variation, yielding the fifth entrie of table 2.3. On the other hand, Peik et al, have measured an optical transition frequency in  $^{171}Yb+$  with a cesium atomic clock. Furthermore, they perform a linear regression analysis using this result toghether with other optical transition frequency measurements [28, 29]. On one hand, a linear regression analysis with three points has no statistical significance. On the other hand, we have already considered the other data. Therefore, we have also reanalyzed the data, using only the comparison between  $Yb+$  and  $Cs$  frequency, yielding the sixth entrie in table 2.3.

## 2.4 Quasar absorption systems

Quasar absorption systems present ideal laboratories to search for any temporal variation in the fundamental constants. The continuum spectrum of a quasar was formed at an epoch corresponding to the redshift  $z$  of main emission details specified by the relationship:

$$\lambda_{obs} = \lambda_{lab} (1 + z). \quad (6)$$

Quasar spectra of high redshift show the absorption resonance lines of alkaline ions like CIV, MgII, FeII, SiIV and others, corresponding to the

Table 2: The table shows the clocks compared, the value of  $\frac{\Delta\alpha}{\alpha}$  and its corresponding error, the time interval for which the variation was measured and the reference.

Frequencies	$\frac{\Delta\alpha}{\alpha}$	$\sigma\left(\frac{\Delta\alpha}{\alpha}\right)$	$\Delta t(\text{yr})$	Reference
Hg+ and H maser	0	$1.4 \cdot 10^{-14}$	0.38	[25]
Cs and Rb	$8.4 \cdot 10^{-15}$	$13.8 \cdot 10^{-15}$	2	[26]
Cs and Rb	$-2 \cdot 10^{-16}$	$8 \cdot 10^{-15}$	5	[27]
Hg and Cs	0	$2.4 \cdot 10^{-15}$	2	[28]
H and Cs	$5.7 \cdot 10^{-15}$	$11.2 \cdot 10^{-15}$	5	[29]
Yb and Cs	$-1.6 \cdot 10^{-15}$	$5.9 \cdot 10^{-15}$	2.8	[30]

$S_{1/2} \rightarrow P_{3/2}(\lambda_1)$  and  $S_{1/2} \rightarrow P_{1/2}(\lambda_2)$  transitions. The relative magnitude of the fine splitting of the corresponding resonance lines is proportional to the square of the fine structure constant  $\alpha$  to lowest order in  $\alpha$ .

$$\frac{\Delta\lambda}{\lambda} = \frac{\lambda_1 - \lambda_2}{\lambda} \sim \alpha^2 \quad (7)$$

Therefore, any change in the value of  $\alpha$  at redshift  $z$  with respect to the laboratory value, can be measured from the separation of the doublets  $\Delta\lambda$  as follows:

$$\frac{\Delta\alpha}{\alpha} = \frac{1}{2}c_r \left[ \frac{\left(\frac{\Delta\lambda}{\lambda}\right)_z}{\left(\frac{\Delta\lambda}{\lambda}\right)_{now}} - 1 \right]$$

where  $c_r$  is a correction term which depends on the ion considered. This method is known in the literature as the Alkali Doublet (AD) method. Several authors have applied this method to SiIV doublet absorption lines systems at different redshifts ( $1 < z < 3.6$ ). We show the average values they obtain in table 3. On the other hand, in order to perform our statistical analysis, we consider the individual data and corresponding errors for each absorption cloud which can be found in the references.

Bahcall et al [41] use strong nebular emission lines of O III to constrain the variation of  $\alpha$ . Again, in this case, measuring the relative separation of the doublet give a constraint on  $\alpha^2$  at a given redshift. Assuming a linear variation of  $\alpha$  with time, the authors find  $\frac{\Delta\alpha}{\alpha} = (-0.7 \pm 1.4) \times 10^{-4}$ . In this work, we want to test a theoretical model and thus the data must be model independent. Thus, we will consider the individual measurements on the variation of  $\alpha$  belonging to the standard sample consisting in 42 quasar absorption systems, which are listed in table 4 of reference [41].

Table 3: The table shows the redshift interval, the average value and standard deviation of  $\frac{\Delta\alpha}{\alpha}$  in units of  $10^{-4}$  obtained using the AD method and the corresponding reference.

$z_{abs}$	$\frac{\Delta\alpha}{\alpha}$ $\times 10^{-4}$	$\sigma\left(\frac{\Delta\alpha}{\alpha}\right)$ $\times 10^{-4}$	Reference
$2.6 < z < 3.6$	-0.35	3.5	[31]
$2.8 < z < 3.05$	0.21	1.4	[32]
$2 < z < 3$	-0.05	0.13	[36]
$1.18 < z < 1.83$	-0.31	0.85	[42]

An improvement to the AD Method was proposed by Webb et al [33, 53]. The new method called in the literature the Many Multiplet (MM) method compares transitions of different species, with widely differing atomic masses together with different transitions of the same species. If we consider a many electron atom or ion, the relativistic correction to the energy of the external electron can be written as:

$$\Delta \sim (Z_n\alpha)^2 |E|^{3/2} \left[ \frac{1}{j+1/2} - C(j,l) \right] \quad (8)$$

where  $Z_n$  is the nuclear charge,  $E$  is the electron's energy,  $j$  and  $l$  are the electrons's total and orbital angular momentum respectively. Moreover,  $C(j,l)$  is the contribution added due to the many body effects. Again, as in the case of the atomic clocks, the relativistic contribution is proportional de  $Z\alpha^2$  and therefore comparing different transitions of the same atom or transitions of different atoms, is a useful tool to put bounds on  $\alpha$ . Moreover, the energy equation for a transition to the ground state, within a particular multiplet, at a redshift  $z$  reads:

$$E_z = E_c + \left[ Q_1 + K_1 (\vec{L} \cdot \vec{S}) \right] Z_n^2 \left[ \left( \frac{\alpha_z}{\alpha_0} \right)^2 - 1 \right] + K_2 (\vec{L} \cdot \vec{S}) Z_n^4 \left[ \left( \frac{\alpha_z}{\alpha_0} \right)^4 - 1 \right] \quad (9)$$

where  $\vec{L}$  and  $\vec{S}$  are the electron total orbital angular and spin momentum respectively,  $E_c$  is the energy of the configuration centre,  $Q_1$ ,  $K_1$  y  $K_2$  are relativistic coefficients which have been accurately computed by Dzuba et al. [53, 54, 55]. The limits over the fine structure constant variation are obtained fitting Voigt profiles to the absorption features in several different transitions. To the three usual fit parameters : column density, Doppler

width and redshift, they add  $\frac{\Delta\alpha}{\alpha}$ . In such way, this method makes possible to gain an order of order of magnitude in sensibility with respect to the AD method. On the other hand, the simultaneous fit of the Voigt profiles, can allow that unknown systematic errors hide under the variation of  $\alpha$ . As mentioned before, this method provides the only results consistent with a time varying fine structure constant [33, 34, 35, 39]. In a recent work [39] they estimate  $\frac{\Delta\alpha}{\alpha} = (-0.543 \pm 0.116) \times 10^{-5}$  for 128 absorption systems over the redshift range  $0.2 < z < 3.7$  confirming their previous results. For our analysis we consider the individual values obtained for each absorption system, listed in table 3 of reference [39]. As suggested by the authors we add to the each individual error listed in table 3 of ref. [39], an additional random error of  $2.09 \times 10^{-5}$ .

On the other hand, the same method was applied by other authors [44, 56], who also use a stringent selection criteria of the samples, discarding weak and blended lines among others. They have obtained no variation of  $\alpha$  for a high quality quasar spectra obtained using VLT over the redshift range  $0.4 < z < 2.3$ . Again, in this case, we use the individual estimates obtained for each redshift listed in table 3 of reference [56]. On the other hand, the standard MM technique can be revised to avoid the deficiencies pointed out earlier and in the literature [41, 57, 43]. In fact, for  $\frac{\Delta\alpha}{\alpha} \ll 1$  equation 9 can be re-written as follows:

$$z_i = z_\alpha + \kappa_\alpha Q_i \quad (10)$$

where  $z_i$  denotes the observed redshift and  $Q_i$  the sensitivity coefficient corresponding to the lines  $i$ , and the slope parameter  $\kappa_\alpha$  is given by:

$$\kappa_\alpha = -2(1 + z_\alpha) \frac{\Delta\alpha}{\alpha} \quad (11)$$

In such way, it is possible to estimate the variation of  $\alpha$  from linear regression analysis of the position of the line centroids in an absorption component. The accuracy of the regression analysis will be improved, if several absorption line samples are combined. This improved method called in the literature as Revised Many Multiplet (RMM) method, was applied by Levshakov [57] and Quast et al [43] to a homogeneous sample of FeII lines at redshift  $z = 1.149$  and  $z = 1.15$  to obtain  $\frac{\Delta\alpha}{\alpha} = (1.1 \pm 1.1) \times 10^{-5}$  and  $\frac{\Delta\alpha}{\alpha} = (-0.4 \pm 4.6) \times 10^{-5}$  respectively.

On the other hand,  $OH$  lines can provide precise constraints on cosmic evolution of  $\alpha$ , the proton  $g$  factor and the ratio of electron to proton mass. Again, in this chapter, we will only consider  $\alpha$  variation. Darling [58] reported the detection of of the satellite 18 cm  $OH$  conjugate lines at 1612

and 1720 MHz in the  $z = 0.2467$  molecular absorption system toward the radio source PKS 1413 + 135. Conjugate lines profiles guarantee that both lines originate in the same molecular gas. On the other hand, the 18 cm  $OH$  lines can be decomposed into a  $\Lambda$ -doubled term which depends weakly on  $\alpha$  and a hyperfine term which has a strong  $\alpha^4$  dependence. From these, sums and differences of lines can form pure  $\Lambda$ -doubled and pure hyperfine quantities:

$$\begin{aligned}\Sigma\nu &= \nu_{1720} + \nu_{1612} = 2\Lambda\alpha^{0.4} \\ \Delta\nu &= \nu_{1720} - \nu_{1612} = 2(\Delta^+ + \Delta^-)\alpha^4\end{aligned}$$

where  $\Delta^+ = 9.720$  MHz and  $\Delta^- = 9.375$  MHz and  $\Lambda = 11926$  MHz. In such way, Darling obtains  $\frac{\Delta\alpha}{\alpha} = (0.5 \pm 1.3) \times 10^{-5}$ .

Moreover, the ratio of the hyperfine 21 cm absorption transition of neutral hydrogen  $\nu_a$  to an optical resonance transition  $\nu_b$  is proportional to  $x = \alpha^2 g_p \frac{m_e}{m_p}$  where  $g_p$  is the proton  $g$  factor. Thus, a change of this quantity will result in a difference in the redshift measured from 21 cm and optical absorption lines as follows:

$$\frac{\Delta x}{x} = \frac{z_{opt} - z_{21}}{(1+z)} \quad (12)$$

So, combining the measurements of optical and radio redshift, a bound on  $\alpha^2$  can be obtained. Table 4 shows the bounds obtained by different authors using this method. This method has the inconvenience that it is difficult to determine if both radio and optical lines originate at the same absorption system. Thus, a difference in the velocity of the absorption clouds could hide in a variation of  $\alpha$ .

The ratio of the rotational transition frequencies of diatomic molecules such as CO to the 21 cm hyperfine transition in hydrogen is proportional to  $y = g_p \alpha^2$ . Thus, any variation in  $y$  would be observed as a difference in the redshifts measured from 21 cm and molecular transition lines:

$$\frac{\Delta y}{y} = \frac{z_{mol} - z_{21}}{(1+z)} \quad (13)$$

Murphy et al. [61] have placed upper limits at redshift  $z = 0.25$ ,  $\frac{\Delta\alpha}{\alpha} = (-0.1 \pm 0.22) \times 10^{-5}$  and at redshift  $z = 0.68$ ,  $\frac{\Delta\alpha}{\alpha} = (-0.08 \pm 0.27) \times 10^{-5}$ .

Table 4: The table shows the absorption redshift, the value and standard deviation of  $\frac{\Delta\alpha}{\alpha}$  obtained comparing optical and radio lines in units of  $10^{-4}$  and the corresponding references

$z_{abs}$	$\frac{\Delta\alpha}{\alpha}$	$\sigma\left(\frac{\Delta\alpha}{\alpha}\right)$	Reference
1.77	-0.035	0.055	[31]
0.52	0	0.6	[59]
0.69	0	1.4	[60]

## 2.5 Cosmic Microwave Background

Any variation of the fine structure constant  $\alpha$  alters the physical conditions at recombination and therefore changes the cosmic microwave background (CMB) fluctuation spectrum. The dominant effect is a change in the redshift of recombination, due to a shift in the energy levels and, in particular the binding energy of Hydrogen. The Thompson scattering cross section is also changed for all particles, being proportional to  $\alpha^2$ . A different value of  $\alpha$  at recombination affects the CMB fluctuation spectrum in two ways: i) a shift in the Doppler peaks position and ii) a change in the amplitude of the Doppler peaks. On the other hand, the CMB fluctuation spectrum is sensitive to many cosmological parameters such as the density of barionic and dark matter, the Hubble constant and the index of primordial spectral fluctuations. Moreover, the effect of changing these parameters is similar to a change in  $\alpha$ . Even though the bounds obtained using this method are not very stringent, it is important to consider a bound of  $\alpha$  in the early universe.

Martins et al [47, 48] have performed an estimation of the fine structure constant together with other cosmological parameters with the first year data of the Wilkinson Anisotropy Probe (WMAP) [62]. They established the following bound:

$$\frac{\Delta\alpha}{\alpha} = 0.025 \pm 0.035 \quad (14)$$

## 3 Theoretical Model

In this section, we review the theoretical model proposed by Damour and Polyakov. We derive the expression for the observable quantity  $\frac{\Delta\alpha}{\alpha}$ , including the renormalization group correction which was not considered in the original paper.

### 3.1 The Gravity-dilaton-matter Model

The existence of a massless scalar field coupled to gravity and matter presents a host of effects that contradicts several experiments. Universal couplings violate the strong equivalence principle while non universal ones violate the universality of free fall for different composite probes. The original proposal of ref [4] was a mechanism by which the dilaton, while still massless, is attracted towards some maximum of its coupling functions to the other fields (denoted as  $B_a$ ). It is known that string loop effects associated with world-sheets of arbitrary genus in intermediate string states can make  $B_a = B_a(\Phi)$  to depend on  $\Phi$  in a non-monotonic way. If the extrema of this functions differ from each other, then the dilaton can still at present be sensitively changing in time, producing unacceptable time dependences of fundamental constants and violation to the weak equivalence principle. Conversely, if the coupling is universal, then the extremum will be universal as well and the cosmological evolution at all stages will conspire to drive the dilaton almost precisely towards such a value, leaving a very tiny remanent time dependence and very small violations of universality of free fall.

Let us briefly describe the model. In the string frame metric denoted as  $\hat{g}_{\mu\nu}$  the dilaton couples in a universal multiplicative way to all other fields at the string tree level. However, when taking the full string-loop expansion, the effective action takes the general form:

$$S = \int d^4x \sqrt{\hat{g}} \left( \frac{B_g(\Phi)}{\alpha'} \hat{R} + \frac{B_\Phi(\Phi)}{\alpha'} [4\Box\Phi - 4(\hat{\nabla}\Phi)^2] - B_F(\Phi) \frac{k}{4} \hat{F}^2 - B_\psi(\Phi) \bar{\psi} \hat{D} \hat{\Psi} - i \bar{\Psi} m_f \hat{\Psi} \right) \quad (15)$$

where  $\hat{R}$  is the Ricci scalar corresponding to the string metric,  $\Phi$  the dilaton,  $\hat{F}^2 = F_{\mu\nu}^a F^{a\mu\nu}$  with  $F_{\mu\nu}^a = \partial_\mu(A_\nu^a) - \partial_\nu(A_\mu^a) + f^{abc} A_\mu^b A_\nu^c$  includes all the gauge fields, and  $\hat{D}$  is the gauge covariant derivative.

Following ref.[4] we introduce the Einstein metric  $g_{\mu\nu} = C B_g(\Phi) \hat{g}_{\mu\nu}$  and a convenient  $\Phi$ -dependent rescaling:

$$\phi = \int d\Phi \left( \frac{3}{4} \left( \frac{B'_g}{B_g} \right)^2 + 2 \frac{B'_\Phi}{B_g} + 2 \frac{B_\Phi}{B_g} \right)^{\frac{1}{2}} \quad (16)$$

where  $B'_g = dB_g/d\Phi$  and  $C$  is a constant such as  $C B_g(\Phi_0) = 1$  today. Also we rescale the Dirac fields:

$$\Psi = C^{-\frac{3}{4}} B_g^{-\frac{3}{4}} B_\Phi^{\frac{1}{2}} \hat{\Psi} \quad (17)$$

finally obtaining the action, decomposed into a gravitational sector  $(g_{\mu\nu}, \phi)$  and a matter sector  $(\psi, A, \dots)$ :

$$S[g, \Phi, \Psi, A, \dots] = S_{g, \Phi} + S_m \quad (18)$$

$$S_{g, \Phi} = \int d^4x \sqrt{\hat{g}} \left( \frac{R}{4q} - \frac{(\nabla\Phi)^2}{2q} \right) \quad (19)$$

$$S_m = \int d^4x \sqrt{\hat{g}} \left( -\bar{\psi} \hat{D} \hat{\Psi} - \frac{k}{4} B_F(\Phi) \hat{F}^2 - i \bar{\Psi} m_f \hat{\Psi} \right) \quad (20)$$

where  $q = 4\pi G$  and  $G$  is Newton's constant (the action does not include de poorly-known Higgs sector). We see that the unified gauge coupling constant is given by:

$$g^{-2} = \alpha_{GUT}^{-1} = k B_F(\Phi), \quad (21)$$

a function of the dilaton. Rescaling the metric means rescaling inversely all energies, so the string cutoff mass scale becomes dilaton dependent in Einstein units:

$$\Lambda_s(\phi) = C^{-1/2} B_g^{-1/2}(\phi) \hat{\Lambda}_s. \quad (22)$$

We still need to land on observational energy scales. In the case of an asymptotically free theory (e.g. QCD), at the one loop level the infrared confinement mass scale  $\Lambda_{conf}$  is related to the cutoff scale as

$$\Lambda_{conf} \propto \Lambda_s \exp(-8\pi^2 b^{-1} g^{-2}) = C^{-1/2} B_g^{-1/2}(\phi) \exp[-8\pi^2 b^{-1} k B_F(\phi)] \hat{\Lambda}_s, \quad (23)$$

with  $b$  dependent on the particular gauge and matter fields.

It is assumed that the mass of any particle  $A$  depends in a non-trivial way on the VEV of the dilaton through the  $B$ s:

$$m_A(\phi) = m_A[B_g(\phi), B_F(\phi), \dots] \quad (24)$$

the key hypothesis of ref.[4] being that the functions  $m_A(\phi)$  all have the same minimum  $\phi_m$  that monotonically drives the dilaton to that value, as mentioned above.

Another key assumption, inspired by Eq.23 and the chiral limit in QCD (all energies proportional to  $\Lambda_{QCD}$ ), is that any mass (composite or not) have the following form:

$$m_A(\phi) = \mu_A B^{-1/2}(\phi) \exp[-8\pi^2 \nu_A B(\phi)] \hat{\Lambda}_s, \quad (25)$$

where it has been assumed that all couplings  $B_i$  depend on a common function  $B$  through functions  $f_i$  (sufficient condition to have a common extremum);  $\nu_A$  and  $\mu_A$  are pure numbers of order unity. From here we see that a minimum of  $m_A(\phi)$  corresponds to a maximum of  $B(\phi)$ , and hence a minimum of  $\ln B^{-1}(\phi)$ . Following [4] we expand this function up to second order around the minimum:

$$\ln B^{-1}(\phi) = \ln B^{-1}(\phi_m) + \frac{1}{2}\kappa(\phi - \phi_m)^2. \quad (26)$$

From Eq.21 we see that  $\ln \alpha_{GUT} \propto \ln B^{-1}$ . In the next section we will study the cosmological model rendering the time dependence of  $\phi$ . Now we focus on the relation between  $\alpha_{GUT}$  and  $\alpha$ . First it is convenient to work at the unification scale  $E_{GUT}$ .  $\alpha$  can be written in terms of the  $U(1) \otimes SU(2)$  coupling constants as:

$$\frac{1}{\alpha(E_{GUT})} = \frac{5}{2} \frac{1}{\alpha_1(E_{GUT})} + \frac{1}{\alpha_2(E_{GUT})} = \frac{7}{2} \frac{1}{\alpha_{GUT}} \quad (27)$$

where we have used that  $\alpha_1(GUT) = \alpha_2(GUT) = \alpha_{GUT}$ , the unification value.

The renormalization group equation for the observable  $\alpha$  is:

$$\frac{1}{\alpha(E_O)} = \frac{7}{2} \frac{1}{\alpha_{GUT}} + \hat{b} \ln \left( \frac{E_{GUT}}{E_O} \right) \quad (28)$$

where  $\hat{b}$  depends on the unification model, and  $E_O$  is the energy at which we measure  $\alpha$ . Given that we expect  $\Delta\alpha/\alpha \leq 10^{-5}$ , we can write:

$$\frac{\Delta\alpha}{\alpha} = \alpha \left( \frac{1}{\alpha_0} - \frac{1}{\alpha} \right) \simeq \alpha_0 \left( \frac{1}{\alpha_0} - \frac{1}{\alpha} \right). \quad (29)$$

From Eq.23, and assuming that  $E_{GUT} \simeq \Lambda_s$ , we expect that:

$$\frac{E_{GUT}}{E_O} = C^{1/2} B_g^{1/2}(\phi) \exp[8\pi^2 b^{-1} k B_F(\phi)]. \quad (30)$$

Consequently we have:

$$\Delta \ln \left( \frac{E_{GUT}}{E_O} \right) = \frac{1}{2} \Delta \ln B_g + 8\pi^2 b^{-1} k \Delta B_F(\phi). \quad (31)$$

Combining the last three equations we obtain:

$$\frac{\Delta\alpha}{\alpha}(t) = \left( \frac{7}{2} + 8\pi^2 \frac{\hat{b}}{b} \right) \alpha_0 \Delta \alpha_{GUT}^{-1} + \frac{\hat{b}}{2} \alpha_0 \frac{\Delta B_g}{B_g}, \quad (32)$$

where  $\alpha_0 = 1/137$  is the present low energy value of the fine structure constant. Under the hypothesis of universality, we have  $B_g(\phi) = B_F(\phi) = B(\phi)$ , and the last equation simplifies to

$$\frac{\Delta\alpha}{\alpha}(t) = \left( \frac{7}{2} + 8\pi^2 \frac{\hat{b}}{b} + \frac{\hat{b}}{2} \right) \alpha_0 \frac{\Delta B}{B} = \mathcal{A} \Delta \ln B^{-1}. \quad (33)$$

We can estimate  $\hat{b}$  from Eq.28 ( $\alpha_{GUT}(t_0) \simeq \frac{1}{50}$ ). Regarding the string one-loop coefficient  $b$  which relates different mass scales, it depends on group parameters of order one (as well as  $\hat{b}$ ) and is positive. As we are seeking upper bounds for the parameter  $\Delta\phi$  from the observational upper bounds on  $\Delta\alpha$ , we will use the conservative lower bound  $\mathcal{A} = 7/2 + \hat{b}/2$ . From Eq.26 we can then write:

$$\frac{\Delta\alpha}{\alpha}(t) = \frac{1}{2} \mathcal{A} \kappa \Delta \{(\phi(t) - \phi_m)^2\}. \quad (34)$$

In order to proceed we must solve the cosmological time evolution of the dilaton, which we do in the next section.

### 3.2 Cosmological Solution

We need to know the time evolution of the dilaton, which will be apparent after solving Einstein equations together with the dilaton equation. The equation derived from the action  $S = S_{g,\Phi} + S_m$  are:

$$R_{\mu\nu} = 2\partial_\mu\phi\partial_\nu\phi + 2q(T_{\mu\nu} - \frac{1}{2}g_{\mu\nu}) \quad (35)$$

$$\square\phi = -q\sigma \quad (36)$$

where

$$T^{\mu\nu} = 2g^{-1/2} \frac{\delta S_m}{\delta g_{\mu\nu}} \quad (37)$$

$$\sigma = 2g^{-1/2} \frac{\delta S_m}{\delta\phi} \quad (38)$$

are the sources.

The several gasses (labeled by  $A$ ) that describe the material content of the Universe, which we supposed weakly interacting, can be written as:

$$T^{\mu\nu} = \frac{1}{\sqrt{g(x)}} \sum_A \int d^4x_A m_A [\phi(x_A)] u_A^\mu u_A^\nu \delta^{(4)}(x - x_A) \quad (39)$$

and consequently

$$\begin{aligned}\sigma(x) &= -\frac{1}{\sqrt{g(x)}} \sum_A \int ds_A \alpha_A[\phi(x_a)] m_A[\phi(x_a)] \delta^{(4)}(x - x_A) \\ &= \sum_A \alpha_A[\phi(x_A)] T_A(x)\end{aligned}\quad (40)$$

where

$$\alpha_A(\phi) = \frac{\delta \ln m_A(\phi)}{\delta \phi} \quad (41)$$

is a measure of the strenght of the dilaton coupling to the  $A$  particles,  $u_A^\mu = dx_A^\mu/ds_A$  and  $T_A = -\rho_A + 3P_A$  is the  $A$  particles contribution to the trace of the energy-momentum tensor.

We consider the Friedmann cosmological model, in which  $ds^2 = -dt^2 + a(t)^2 dl^2$  where  $dl^2 = (1 - Kr^2)^{-1} dr^2 + r^2(d\theta^2 + \sin^2\theta d\phi^2)$  with  $K = 0, 1, -1$ . Thus the gravitational and dilaton field equations simplify to:

$$\begin{aligned}-3\frac{\dot{a}}{a} &= q(\rho + 3P) + 2\dot{\phi}^2 \\ 3H^2 + 3\frac{K}{a^2} &= 2q\rho + \dot{\phi}^2 \\ \ddot{\phi} + 3H\dot{\phi} &= q\sigma\end{aligned}\quad (42)$$

where the dot denotes the time derivative ( $d/dt$ ) and  $H = \dot{a}/a$ . We focus on the flat case  $K = 0$ . Combining eqs. 42 and working with the logarithmic time  $p = \ln a + cte$  we have:

$$\frac{2}{(3 - \phi'^2)} \phi'' + (1 - \lambda)\phi' = \frac{\sigma}{\rho} \quad (43)$$

where  $\lambda = P/\rho$ .

In Ref.[4] it is analyzed both the radiation and the matter dominated eras, with no cosmological constant. Even though most of the data, belong to the  $\Lambda$  dominated era, we assume that the expressions for the evolution of the dilaton field will be similar. Therefore, we concentrate on the matter era, leaving the case with cosmological constant to another work. After decoupling, there is no interaction between matter and radiation cosmologically important, so we have  $\rho = \rho_m + \rho_r$ ,  $P = P_r + P_m$ ,  $\sigma = -\alpha_m(\phi)(\rho_m - 3P_m)$  with  $P_r = \frac{1}{3}\rho_r$ ,  $P_m \simeq 0$  and  $\alpha_m(\phi) = \frac{\partial \ln m_m(\phi)}{\partial \phi}$ .

The noninteracting relativistic and non relativistic components satisfy respectively  $\rho_r \propto a^{-4}$  and  $\rho_m \propto m_m(\phi)a^{-3}$ . The evolution equation can be finally written as:

$$\frac{2}{(3 - \phi'^2)}\phi'' + (1 - \lambda(p, \phi))\phi' = -[1 - 3\lambda(p, \phi)]\alpha_m(\phi) \quad (44)$$

where

$$3\lambda(p, \phi) = [1 + Cm_m(\phi)e^p]^{-1} \quad (45)$$

In the analysis of [4] it was concluded that the radiation era is very efficient in attracting the dilaton very near its minimum  $\phi_m$ , and so we can approximate  $m_m(\phi) \simeq const$  in  $\lambda(p, \phi)$ . We choose the origin of  $p$  at matter-radiation equality  $\rho_r(p = 0) = \rho_m(p = 0)$ ,  $\lambda(0) = 1/3\rho_r(0)/(\rho_r(0) + \rho_m(0)) = 1/6$ . Consequently  $C = m_m^{-1}$  and  $\lambda(p) = \frac{1}{3}(1 + e^p)^{-1}$ .

From Eqs.(25,26) we obtain

$$\alpha_A(\phi) = \beta_A(\phi - \phi_m) \quad (46)$$

where

$$\beta_A = \kappa(40.75 - \ln(\frac{m_A}{1\text{Gev}})) \quad (47)$$

and we have used the values as in Ref.[4]. Even though we will take for  $m_A = 1$  GeV, the mass of the nucleon, the dark matter case  $m = 40$  GeV would only change logarithmically the value of  $\beta$ . Neglecting  $\phi'^2$  in Eq.44 we obtain:

$$\frac{2}{3}\phi'' + (1 - \lambda(p))\phi' = -[1 - 3\lambda(p)]\beta_m(\phi - \phi_m) \quad (48)$$

Denoting  $x = e^p = a/a_{equivalence}$  we have

$$(1 + x)x\partial_x^2\phi + (\frac{5}{2}x + 2)\partial_x\phi + \frac{3}{2}\beta_m(\phi - \phi_m) = 0. \quad (49)$$

This is a hypergeometric-type differential equation, with the condition of regularity  $\phi(x = 0) = \phi_{rad}$ , being  $\phi_{rad}$  the value of  $\phi$  at the end of the radiation era. The parameters are

$$\begin{aligned} z &= -x \\ \alpha &= \frac{3}{4} - iw \\ \beta &= \frac{3}{4} + iw \end{aligned}$$

$$\gamma = 2$$

with  $w = \frac{3}{2}(\beta_m - 3/8)^{1/2}$ . The solution then reads

$$\phi - \phi_m = (\phi_{rad} - \phi_m) F(\alpha, \beta, \gamma; -x) \quad (50)$$

with

$$F_m(\alpha, \beta, \gamma; -x) = \frac{\phi(x) - \phi_m}{\phi_{rad} - \phi_m} \quad (51)$$

As the argument is the red-shift, for high values we can use the asymptotic behaviour of  $F_m$ . Unless  $\kappa$  has the unnatural value  $9.2 \times 10^{-3}$  or less, the sign of  $\beta_m - 3/8$  will be positive, which we will assume. Then  $\omega$  is real and we have:

$$F_m(\kappa, t) = \left[ \frac{\coth(2\pi\omega)}{\pi\omega(\omega^2 + \frac{1}{16})} \right]^{1/2} \exp(-\frac{3}{4}p) \cos \theta \quad (52)$$

where  $\theta(t) = \omega p(t) + 2\omega \ln 2 + \text{Arg}\Gamma_2$  with  $\Gamma_2 = \Gamma(2i\omega)/\Gamma(2i\omega + \frac{3}{2})$  and  $p = \ln(a(t)/a_{eq})$ . Defining

$$F_r(\kappa) = \frac{\phi_{rad} - \phi_m}{\phi_i - \phi_m} \quad (53)$$

the attraction factor during the radiation era, whose value is estimated to be  $1.87 \times 10^{-4} \times \kappa^{-9/4}$  (see Ref[4]) and

$$\Delta\phi = \phi_i - \phi_m \quad (54)$$

with  $\phi_i$  the ‘‘initial’’ (at some time  $t_i$ ) value of the dilaton, we can write the solution for  $\phi$  as:

$$\phi(t) - \phi_m = F_m(\kappa, t) F_r(\kappa) \Delta\phi \quad (55)$$

or more explicitly:

$$\phi(t) - \phi_m = 1.87 \times 10^{-4} \times \kappa^{-9/4} \left[ \frac{\coth(2\pi\omega)}{\pi\omega(\omega^2 + \frac{1}{16})} \right]^{1/2} \left( \frac{a(t)}{a_{eq}} \right)^{-\frac{3}{4}} \cos \theta(t) \Delta\phi \quad (56)$$

### 3.3 Observational Adjustment

Although it is tempting to work up to first or second order while analyzing Eq.34, this cannot be done as we consider data spanning times comparable to the Hubble time. This makes the Taylor expansion of the function  $\phi(t)$  meaningless. We will be forced then to make a non linear adjustment as we will see below.

We replace the solution found in the previous section into Eq.34, obtaining (our convention for  $\Delta$  is  $\Delta f(t) \equiv f(t) - f(t_0)$ )

$$\frac{\Delta\alpha}{\alpha}(t) = 1.75 \times 10^{-8} \mathcal{A} \kappa^{-7/2} (\Delta\phi)^2 \mathcal{C}(\kappa) \Delta\mathcal{D}(\kappa, t), \quad (57)$$

where we have defined the functions

$$\mathcal{C}(\kappa) = \frac{\coth(2\pi\omega)}{\pi\omega(\omega^2 + \frac{1}{16})} \quad (58)$$

and

$$\mathcal{D}(\kappa, t) = \left( \frac{a(t)}{a_{eq}} \right)^{-3/2} \cos^2(\theta(t)). \quad (59)$$

This entails a nonlinear adjustment of the parameters  $\kappa^{-7/2}(\Delta\phi)^2$  and  $\kappa$ .

Finally, it is important to note that not all data were fitted to eq. 57. Actually the data obtained from experiments with atomic clocks provide stringent bounds on  $\frac{\dot{\alpha}}{\alpha}$ . Therefore, if we fit the derived quantity  $\frac{\Delta\alpha}{\alpha}$ , the fitting procedure and results will be almost dominated by these data. Thus we consider the following expression for the actual data on the variation of  $\alpha$  [4]:

$$\frac{\dot{\alpha}}{\alpha} = -\kappa H_0 \left( \omega \tan \theta(t_0) + \frac{3}{4} \right) \left[ 1.87 \times 10^{-4} \kappa^{-9/4} F_m(\kappa, t_0) \Delta\phi \right]^2 \quad (60)$$

## 4 Results and Discussion

We have performed a statistical analysis working on a  $\chi^2$  function to compute the best-fit parameter values and uncertainties. For the 246 data described in section 2, we obtain  $\chi_{min}^2 = 357$ . However, we have analyzed the contribution of each data to  $\chi^2$  and found that only 6 data have an enourmous contribution while the contributions of the other 240 are of order 1 or less. Furthermore, excluding these data, we obtain  $\chi_{min}^2 = 240$  for 240 data and 2 free parameters with no change in the value of the best fit parameters

and errors. Therefore, we excluded these data from the statistical analysis, using what we call the reduced data set. The contours of the likelihood functions in regions of 68 %, 95 % and 99 % of confidence level are shown in figure 1. Unfortunately, the contours do not close, even if we increase the values of  $\kappa$ . This is due to the fact that for increasing  $\kappa$ ,  $\Delta\phi$  has to be increased in order to fit the reduced data set (see eqs. 57, 60). However from figure 1 we can find the following relation between the values of  $\kappa$  and  $\Delta\phi$ , that provide a good fit to the reduced data set.

$$- 3.4 \times 10^{-6} \kappa < \Delta\phi < 3.4 \times 10^{-6} \kappa \quad (61)$$

On the other hand, table 5 shows constraints on the values of  $\Delta\phi$  for fixed values of  $\kappa$ . Again, the values show how increasing values of  $\kappa$ , allow increasing values of  $\Delta\phi$  in order to fit the reduced data set.

We conclude that the string dilaton model proposed by Damour and Polyakov is able to fit almost all experimental and observational data on time variation of the fine structure constant. However, the constraints obtained on the free parameters (considering one or two free parameters) show that  $\Delta\phi = 0$  is also consistent with the data and in this case the model predicts no variation of gauge coupling constants or masses of elementary particles. Nevertheless, it should be noted that in any grand unified theory the variation of the fine structure constant is connected to the variation of the strong coupling constant. Thus, the prediction of this model should also be checked together with the bounds on the strong coupling constant [38, 40]. Furthermore, the data considered in section 2 should be reanalyzed in order to relate the observational values with variations in both the fine structure constant and the strong coupling constant. This requires a more detailed analysis of the QCD model considered and therefore we leave it for future work.

Table 5: The table shows for fixed values of  $\kappa$ , the best fit value and the corresponding  $1\sigma$  error of  $\Delta\phi$

$\kappa$	$\Delta\phi$	$\sigma(\Delta\phi)$
0.01	$2.4 \times 10^{-14}$	$2.3 \times 10^{-13}$
0.1	$-1.0 \times 10^{-10}$	$8.0 \times 10^{-10}$
1	$-4.2 \times 10^{-8}$	$3.2 \times 10^{-7}$
10	$3.6 \times 10^{-6}$	$2.7 \times 10^{-5}$

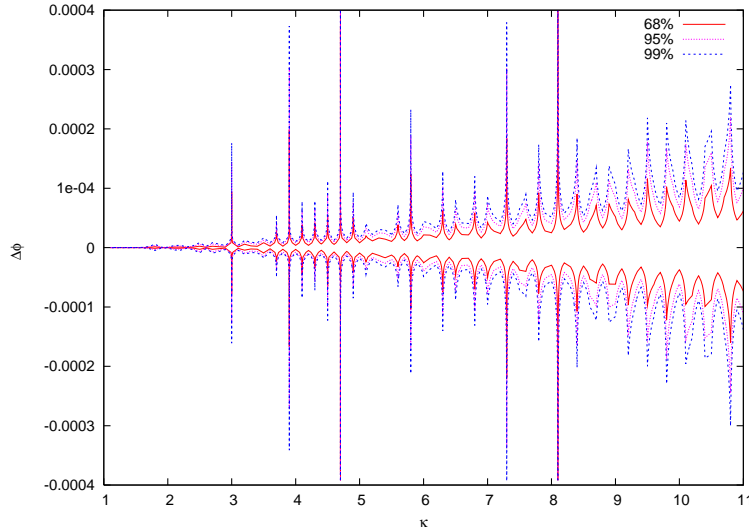


Figure 1: Confidence contours for the free parameters of the DP dilaton model

## 5 Acknowledgements

S. Landau wants to thank M. Murphy for early release of data and useful comments and A.Ivanchik for useful comments.

## References

- [1] Y. Wu and Z. Wang, *Physical Review Letters* **57**, 1978 (1986).
- [2] K. Maeda, *Modern Physics. Letters A* **31**, 243 (1988).
- [3] S. M. Barr and P. K. Mohapatra, *Physical Review D* **38**, 3011 (1988).
- [4] T. Damour and A. M. Polyakov, *Nuclear Physics B* **95**, 10347 (1994).
- [5] T. Damour, F. Piazza, and G. Veneziano, *Physical Review Letters* **89**, 081601 (2002).
- [6] T. Damour, F. Piazza, and G. Veneziano, *Physical Review D* **66**, 046007 (2002).
- [7] D. Youm, *Physical Review D* **63**, 125011 (2001).

- [8] D. Youm, *Physical Review D* **64**, 085011 (2001).
- [9] G. A. Palma, P. Brax, A. C. Davis, and C. van de Bruck, *Physical Review D* **68**, 123519 (2003).
- [10] P. Brax, C. van de Bruck, A.-C. Davis, and C. S. Rhodes, *Astrophysical Journal Supplement* **283**, 627 (2003).
- [11] T. Kaluza, *Sitzungber. Preuss. Akad. Wiss.K* **1**, 966 (1921).
- [12] O. Klein, *Z. Phys.* **37**, 895 (1926).
- [13] S. Weinberg, *Physics Letters B* **125**, 265 (1983).
- [14] M. Gleiser and J. G. Taylor, *Physical Review D* **31**, 1904 (1985).
- [15] J. M. Overduin and P. S. Wesson, *Phys. Rep.* **283**, 303 (1997).
- [16] J. D. Bekenstein, *Physical Review D* **25**, 1527 (1982).
- [17] J. D. Barrow, H. B. Sandvik, and J. Magueijo, *Physical Review D* **65**, 063504 (2002).
- [18] N. Chamoun, S. J. Landau, and H. Vucetich, *Physics Letters B* **504**, 1 (2001).
- [19] T. Damour and F. Dyson, *Nuclear Physics B* **480**, 37 (1996).
- [20] Y. Fujii et al., *Nuclear Physics B* **573**, 377 (2000).
- [21] Y. Fujii et al., *Nuclear Data in Oklo and Time-Variability of Fundamental Coupling Constants*, hep-th/0205206, 2002.
- [22] F. Dyson, *Physical Review Letters* **19**, 1291 (1966).
- [23] P. Sisterna and H. Vucetich, *Physical Review D* **41**, 1034 (1990).
- [24] M. Smolliar, *Science* **271**, 1099 (1996).
- [25] J. D. Prestage, R. L. Tjoelker, and L. Maleki, *Physical Review Letters* **74**, 3511 (1995).
- [26] Y. Sortais et al., *Physica Scripta* **T95**, 50 (2000).
- [27] H. Marion et al., *Physical Review Letters* **90**, 150801 (2003).
- [28] S. Bize et al., *Physical Review Letters* **90**, 150802 (2003).

- [29] M. Fischer et al., *Physical Review Letters* **92**, 230802 (2004).
- [30] E. Peik et al., *New limit on the present temporal variation of the fine structure constant*, physics/0402132, 2004.
- [31] L. L. Cowie and A. Songaila, *Astrophysical Journal* **453**, 596 (1995).
- [32] D. A. Varshalovich, V. E. Panchuk, and A. V. Ivanchik, *Astronomy Letters* **22**, 6 (1996).
- [33] J. K. Webb, V. V. Flambaum, C. W. Churchill, M. J. Drinkwater, and J. D. Barrow, *Physical Review Letters* **82**, 884 (1999).
- [34] J. K. Webb et al., *Physical Review Letters* **87**, 091301 (2001).
- [35] M. T. Murphy et al., *Monthly Notices of the Royal Astronomical Society* **327**, 1208 (2001).
- [36] M. T. Murphy, J. K. Webb, V. V. Flambaum, J. X. Prochaska, and A. M. Wolfe, *Monthly Notices of the Royal Astronomical Society* **327**, 1237 (2001).
- [37] S. A. Levshakov, M. Dessauges-Zavadsky, S. D'Odorico, and M. P., *Monthly Notices of the Royal Astronomical Society* **333**, 373 (2002).
- [38] A. Ivanchik, P. Petitjean, E. Rodriguez, and D. Varshalovich, *Astronomy Letters* **28** (2002).
- [39] M. T. Murphy, J. K. Webb, and V. V. Flambaum, *Monthly Notices of the Royal Astronomical Society* **345**, 609 (2003).
- [40] A. Ivanchik, P. Petitjean, E. Rodriguez, and D. Varshalovich, *Astrophysical Journal Supplement* **283**, 583 (2003).
- [41] J. N. Bahcall, C. L. Steinhardt, and D. Schlegel, *Astrophysical Journal* **600**, 520 (2004).
- [42] A. F. Martínez Fiorenzano, G. Vladilo, and P. Bonifacio, *Societa Astronomica Italiana Memorie Supplement* **3**, 252 (2003).
- [43] R. Quast, D. Reimers, and S. A. Levshakov, *Astronomy and Astrophysics* **415**, L7 (2004).
- [44] R. Srianand, H. Chand, P. Petitjean, and B. Aracil, *Physical Review Letters* **92**, 121302 (2004).

- [45] R. A. Battye, R. Crittenden, and J. Weller, *Physical Review D* **63**, 043505 (2001).
- [46] P. P. Avelino, C. J. A. P. Martins, G. Rocha, and P. Viana, *Physical Review D* **62**, 123508 (2000).
- [47] C. J. Martins et al., *Physical Review D* **66**, 023505 (2002).
- [48] G. Rocha et al., *New Astronomy Review* **47**, 863 (2003).
- [49] L. Bergström, S. Iguri, and H. Rubinstein, *Physical Review D* **60**, 45005 (1999).
- [50] K. Ichikawa and M. Kawasaki, *Phys. Rev.* **D65**, 123511 (2002).
- [51] K. M. Nollet and R. E. Lopez, *Phys. Rev.* **D66**, 063507 (2002).
- [52] P. Sisterna and H. Vucetich, *Physical Review D* **44**, 3096 (1991).
- [53] V. A. Dzuba, V. V. Flambaum, and J. K. Webb, *Physical Review Letters* **82**, 888 (1999).
- [54] V. A. Dzuba, V. V. Flambaum, and J. K. Webb, *Physical Review A* **59**, 230 (1999).
- [55] V. A. Dzuba, V. V. Flambaum, M. T. Murphy, and J. K. Webb, *Physical Review A* **63**, 042509 (2001).
- [56] H. Chand, R. Srianand, P. Petitjean, and B. Aracil, *Astronomy and Astrophysics* **417**, 853 (2004).
- [57] S. Levshakov, *Astrophysical constraints on hypothetical variability of fundamental constants*, astro-ph/0309817, 2003.
- [58] J. Darling, *A Laboratory for Constraining Cosmic Evolution of the Fine Structure Constant: Conjugate 18 cm OH Lines Toward PKS 1413+135 at  $z=0.2467$* , astro-ph/0405240, 2004.
- [59] A. M. Wolfe, R. L. Brown, and M. S. Roberts, *Physical Review Letters* **37**, 179 (1976).
- [60] H. Spinrad and C. F. McKee, *Astrophysical Journal* **232**, 54 (1979).
- [61] M. T. Murphy et al., *Monthly Notices of the Royal Astronomical Society* **327**, 1244 (2001).
- [62] C. L. Bennett et al., *Astrophysical Journal Supplement* **148**, 1 (2003).